Synthesis and Fluorescence Ion-Sensory Properties of the First Dehydropyridoannulene-Type Cyclophane with Enforced Exotopic Metal Ion Binding Sites

Paul. N. W. Baxter*[+][a]

Abstract: The new twistophane **4** has been synthesised, which comprises a conjugated dehydropyridoannulene-type macrocyclic scaffold with outwardly projecting nitrogen-donor sites for the purpose of metal ion coordination. The macrocyclíc structure of **4** was assigned by using spectroscopic methods, and shown to exist in a twisted and chiral ground state conformation by semi-empirical theoretical calculations. A detailed spectroscopic investigation into the metal ion binding properties of **4** and precursor **11** revealed that they functioned as selective complexants, affording a fluorescence quenching output response characteristic of Pd^{II} and Hg^{II} ions. Furthermore, **4** also signalled the presence of Fe^{II}, Co^{II}, Ni^{II} and Ag^{I} ions by the precipitation of coordination polymers, and exhibited reversible proton-triggered fluorescence quenching behaviour. Macrocycle **4** thus represents a unique type of molecular sensory platform, which may find a wealth of potential applications such as the detection of heavy-metal pollutants, as well as for the fabrication of proton-switchable materials and coordination polymers with novel electronic and magnetic properties.

Keywords: alkynes · cyclooligomerization · cyclophanes · macrocyclic ligands · sensors

Introduction

Cyclic macromolecular architectures incorporating ethyne groups as integral structural units, are currently the focus of intense research activity within the domain of macrocyclic and supramolecular chemistry.[1] The first synthetic explorations into the creation of macrocycles involved the preparation of medium-sized rings in which ethyne linkages functioned as pivotal structural components.[2a–c] However, despite the success of these initial studies, ethynyl macrocycles only became the subject of widespread interest nearly 80 years after Ruggli's pioneering investigations.

The late 1980s to early 1990s, witnessed an explosive renewal of interest in the area of ethynyl chemistry and high-carbon content materials, primarily as a result of the discovery and isolation of carbon buckyballs and nanotubes.[3] The syntheses of ethynyl cyclophanes have played a central role in these revived studies, as they serve as potential starting substrates for the generation of fullerenes,[4a–d] carbon nanotubules,[5] carbon networks[6a–d] and nanostructures.[7a, b] Ethynyl cyclophanes now constitute a large and diverse class of macrocyclic architectures comprising for example, expanded radialenes,[8a, b] [*n*]pericyclynes,[1, 9a, b] [*n*]rotanes, exploded [*n*]rotanes,[1, 10a–b] annulenes[11a–c] and dehydroannulenes.[1, 12a–d] Some of these substrates have also been demonstrated to exhibit potentially useful properties such as solid-state porosity,[13a, b] liquid crystallinity,[14] and energy storage capabilities.[1, 5, 10a, b]

With respect to physicochemical properties, the dehydrotetrabenzoannulene-type cyclophanes are particularly interesting as they combine a suite of unique structural features such as, i) cyclic *ortho*-conjugation, ii) a central flattened void for possible guest inclusion, iii) semi-flexibility with hinged molecular motion, and iv) chirality.[15a–g] An especially intriguing avenue of investigation would therefore be to incorporate sites into the dehydroannulene framework for the purpose of metal ion complexation.[16a, b] Materials of this type may be expected to display a rich variety of exploitable properties such as electrochemical, photochemical, magnetic, optical, catalytic, mechanical and sensory abilities.[17a–f]

In earlier work, initial investigations into the above-mentioned possibilities focused upon the synthesis of structures **1** and **2**, which incorporate 2,2′-bipyridyl chelating subunits into a dehydrotetrabenzoannulene scaffold.[16a,b] It was anticipated that binding of metal ions to the pyridine nitrogen atoms would cause perturbations in the electron density distribution over the conjugated macrocyclic scaffold. This in turn would result in alterations of inherent properties such as electrochemical potentials and fluorescence. The

[a] Dr. P. N. W. Baxter[+]
Laboratoire de Chimie Supramoléculaire, Institut Le Bel
Université Louis Pasteur
4 rue Blaise Pascal, 67000 Strasbourg (France)
Fax: (+33) 3-90-24-11-17
E-mail: pbaxter@chimie.u-strasbg.fr
[+] Current address: Institut Charles Sadron, 6 Rue Boussingault, 67083 Strasbourg (France)

 DOI: 10.1002/chem.2003044561

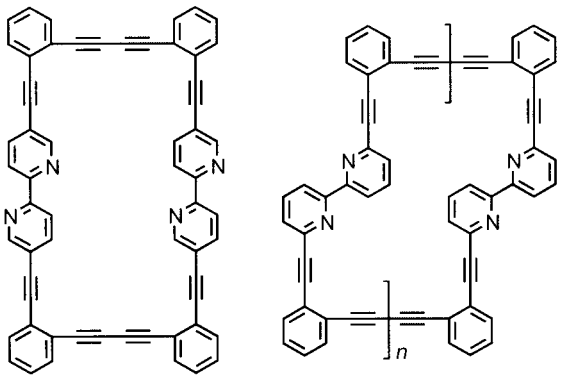

1 **2** : $n = 1$
3 : $n = 2$

complexation of metals to the macrocyclic framework may therefore be detectable instrumentally, and such materials may thus function as spectroscopic ion sensors.[18a–f] Subsequent experimental investigations into the metal ion binding behaviour of **1**, **2** and the structurally related analogue **3**, supported the above expectation. Cyclophane **1** was found to be a selective chromogenic fluorescence sensor for Zn^{II} ions. Ligands **2** and **3** functioned as fluorescence sensors for Cu^{II} ions and protons.[16a, b] The large difference in the observed ion-sensory selectivity between **1**, **2** and **3** was attributed to the differences in structural preorganisation of the respective macrocyclic frameworks.

To further evaluate the potential that cyclic conjugated macrocycles may offer as a structurally new lead class of ion-sensory materials, twistophane **4** was synthesised (Scheme 1).[19] Twistophane **4** differs significantly from **1**, **2** and **3** in that the metal ion binding sites are no longer chelating and incorporated as bridging units. The ion-complexation sites instead comprise 3,4-diethynylpyridine subunits located at the four corners of the macrocycle.[20a, b] The pyridine nitrogen lone pair electrons in **4** project outwardly and away from the central macrocyclic cavity and therefore serve as enforced exotopic metal ion binding sites. As a result, the ion-complexation profile and fluorescence sensory properties of **4** may be expected to be completely different to those of **1**–**3**. In particular, **4** may be capable of forming coordination polymers with certain metal ions.

Herein is described the successful preparation of **4**, which represents the first example of a dehydropyridoannulene-type macrocyclic scaffold with enforced exotopic ion-coordination sites, and a detailed investigation into its ion-binding and sensory behaviour.[21a–e] The latter studies revealed that **4** did indeed form coordination polymers, thereby acting as a precipitation sensor for a small group of transition metals. Twistophane **4** also functioned as a particularly selective fluorescence quenching sensor for Hg^{II} ions and $PdCl_2$.

Results and Discussion

Synthesis of 4: Cyclophane **4** was prepared by using a six-step synthesis in 19% overall yield starting from 3-bromopyridine **5**, and at a later stage in the preparation, 1,4-diethynylbenzene **10** (Scheme 1). The key building block, 3-bromo-4-iodopyridine **6**, was particularly important as it would enable the correct sequence of ethynyl homologations to be achieved during the construction of **4**. Compound **6** has been synthesised by a four-step procedure starting from **5**.[22a, b] Thus **5** was

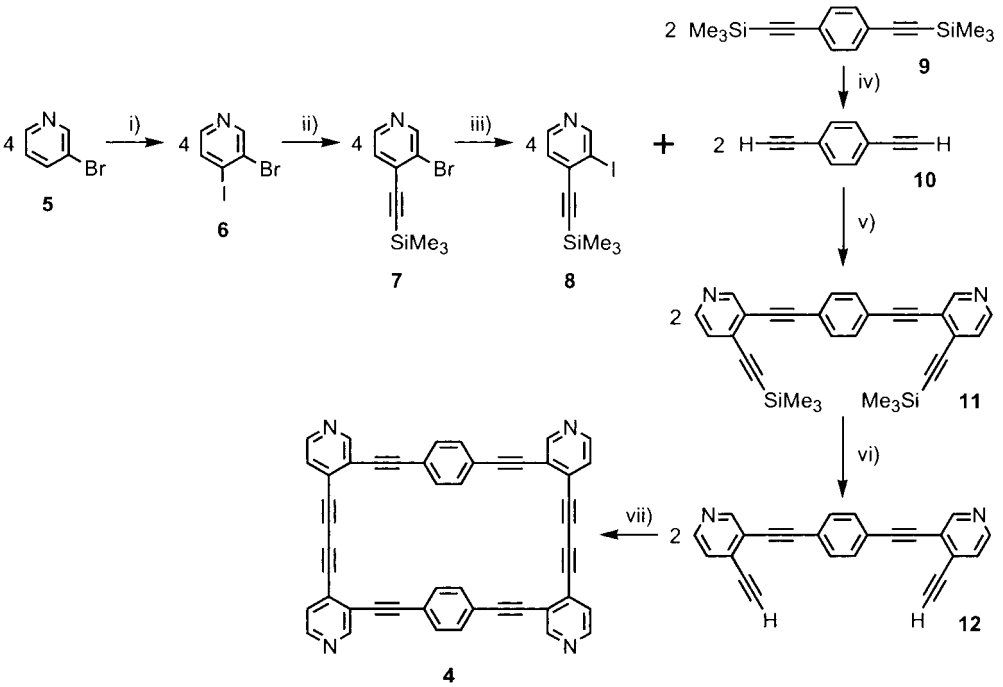

Scheme 1. Synthesis of macrocycle **4**. i) LDA, THF, −80 to −85 °C, 0.75 h, then I_2/THF, −78 °C, 4 h (69%); ii) TMSA, $[PdCl_2(PPh_3)_2]$, CuI cat., Et_3N, 20 °C, seven days (91%); iii) *n*BuLi, Et_2O, −78 °C, 1 h, then ICH_2CH_2I/Et_2O, −78 °C, 2.5 h (86%); iv) K_2CO_3, MeOH, 16 h; v) $[PdCl_2(PPh_3)_2]$, CuI cat., THF, Et_3N, 20 °C, seven days (56%); vi) 1M $(nBu)_4NF$, THF, H_2O, 20 °C, 20 h (88%); vii) $[Cu_2(OAc)_4]$, pyridine, 20 °C, 14 days (71%).

oxidised to the *N*-oxide, and the latter sequentially nitrated, reduced and finally diazotised and iodinated to give **6** in low overall yield. Compound **6** has also been recently synthesised from **5** by regioselective deprotonation with lithium di-*tert*-butyldiisopropylaminozincate (DA-zincate), followed by quenching with iodine.[22c] Pyridine **5** has however been reported to undergo regioselective deprotonation in the 4-position using lithium diisopropylamide (LDA) in THF at low temperature, thereby generating 3-bromo-4-lithiopyridine.[23] It was therefore anticipated that the latter, simpler methodology may provide rapid access to **6**, after quenching the lithiopyridine intermediate with iodine. The LDA-mediated ortholithiation/iodine quench protocol was subsequently found to successfully afford **6** in 69% yield after workup, provided that the reaction temperature was maintained below $-80\,^{\circ}C$. At higher temperatures, considerably reduced yields of **6** accrued, due to side reactions and partial decomposition of the 3-bromo-4-lithiopyridine. Precursor **6** then readily underwent a Sonogashira coupling reaction with trimethylsilylacetylene (TMSA) in Et_3N, using $[PdCl_2(PPh_3)_2]$ as catalyst and CuI as co-catalyst.[24] The ethynylation occurred completely chemoselectively to give **7** in 91% yield. Treatment of **7** with *n*-butyllithium in Et_2O at low temperature resulted in an efficient halogen/lithium exchange reaction. Quenching of the lithiopyridyl intermediate with diiodoethane gave **8**, which was isolated in 86% yield as a heat-sensitive oil. When iodine was used in place of diiodoethane in the latter reaction, significantly reduced yields of **8** were obtained along with 4-trimethylsilylpyridine. Commercial **9** was then deprotected to give **10**,[25a, b] and the latter reacted with two equivalents of **8**, in 12% Et_3N/THF under similar conditions as those employed for the alkynylation of **6**, to provide **11** in 56% yield after purification. If the coupling of **8** with **10** was performed in pure Et_3N, then the desired **11** was isolated along with a significant amount of a contaminant, which was generated by the slow copper-catalysed oxidative dimerisation of the 1:1 **8**+**10** reaction intermediate. The latter intermediate presumably precipitated due to its lower solubility in Et_3N, thereby halting the second ethynylation step. Compound **11** was then cleanly desilylated with excess tetrabutylammonium fluoride (TBAF) in aqueous THF, to furnish dialkyne **12** in 88% yield. Having successfully obtained precursor **12**, the macrocyclisation step to **4** could finally be undertaken.

Previous ethyne-coupling macrocyclisations to give **1**–**3** suggested that cyclisation yields were strongly influenced by the coordination of the precursor bipyridine subunits to the CuCl catalyst, and/or other copper species generated therefrom.[16a–b] Although the pyridines of **12** would be expected to participate in a much weaker metal-binding interaction than those of **1**–**3**, there existed a small chance that the possible formation of coordination oligomers and polymers between CuCl and **12** would negatively influence the yield of **4**. It was therefore decided to explore the effectiveness of the Eglinton/Galbraith ethyne-coupling protocol in the cyclisation of **12**, which uses $[Cu_2(OAc)_4]$ in place of CuCl.[26] Rewardingly, the cyclisation of **12** under medium/high dilution conditions in degassed pyridine with an excess of $[Cu_2(OAc)_4]$ proceeded particularly efficiently, giving **4** in 71% yield after workup.[27]

Characterisation and properties of 4: The structure of the product isolated from the $[Cu_2(OAc)_4]$-mediated coupling of **12** was established to be that of the macrocyclic architecture **4** (Scheme 1) on the basis of mass spectrometric, IR, ^1H and ^{13}C NMR spectroscopic studies.

The FAB mass spectrum of the coupling product recorded in 10% $CF_3COOH/CHCl_3$ displayed a single isotope cluster peak at m/z 653, corresponding exactly to that calculated for the $[M^+ + H]$ isotopic envelope of macrocycle **4**. This structural assignment was further substantiated by a high-resolution FAB mass spectrometric measurement of the $[M^+ + H]$ isotopic envelope, which confirmed the exact elemental composition of the product to be $C_{48}H_{21}N_4$ in accordance with the macrocyclic structure **4** plus one hydrogen.

The IR spectrum of the coupling product of **12** was also supportive of the macrocyclic structural assignment of **4**, in that vibrational modes characteristic of the $\nu(H{-}C{\equiv})$ stretch of terminal alkynes were completely absent. This result establishes that the coupling product is in fact macrocyclic, and not a linear oligomer with unreacted terminal ethyne groups.

The ^{13}C NMR spectrum of the coupling product of **12** comprised eleven peaks, consistent with the above macrocyclic structural assignment. The chemical shifts of the four peaks at $\delta = 97.3 - 80.3$ ppm correspond to the chemically and magnetically inequivalent carbon atoms of two unsymmetrically substituted alkyne groups, and the remaining seven to inequivalent carbon atoms of aromatic rings.

The ^1H NMR spectrum of the coupling product of **12**, also displayed four resonances expected for the macrocyclic structure **4**. A $^1H-^1H$ COSY measurement also verified that it was a single compound and not a mixture of species. Peaks originating from the protons of terminal ethynes were completely absent in the ^1H NMR spectrum of the coupling product, lending further support for the macrocyclic identity of this compound.

Spectral assignments were made on the basis of coupling constants and comparisons with the spectra of **6**–**8**, **11** and **12**. The singlet at $\delta = 8.786$ ppm and the doublet at $\delta = 8.569$ ppm were the furthest downfield resonances in the ^1H NMR spectrum of **4**. They were therefore assigned to the pyridyl H2 and H6 protons, respectively, due to their proximity to the electron-withdrawing pyridine nitrogen atom. The upfield doublet of doublets at $\delta = 7.425$ ppm was thus assigned to the remaining pyridyl H5 proton. Interestingly, the singlet at $\delta =$ 7.336 ppm, which was assigned to the bridging phenyl ring protons of **4**, was significantly upfield-shifted compared to those of **11** and **12** by $\Delta\delta = 0.233$ and 0.242 ppm, respectively. On the other hand, the pyridine protons of **4** are all situated slightly downfield compared to the corresponding protons of **11** and **12** (Figure 1). The upfield-shifting of the phenyl ring protons of **4** is also consistent with its macrocyclic structural assignment. Such a shielding effect would be expected for protons situated within a macrocyclic cavity and/or lying in close proximity to the face of an adjacent aromatic ring.

A semi-empirical AM1 molecular modelling calculation performed upon the macrocyclic structure assigned to **4** also substantiated the latter conclusion (Figure 2).[28a] The modelling studies showed that the ground-state conformation of **4**

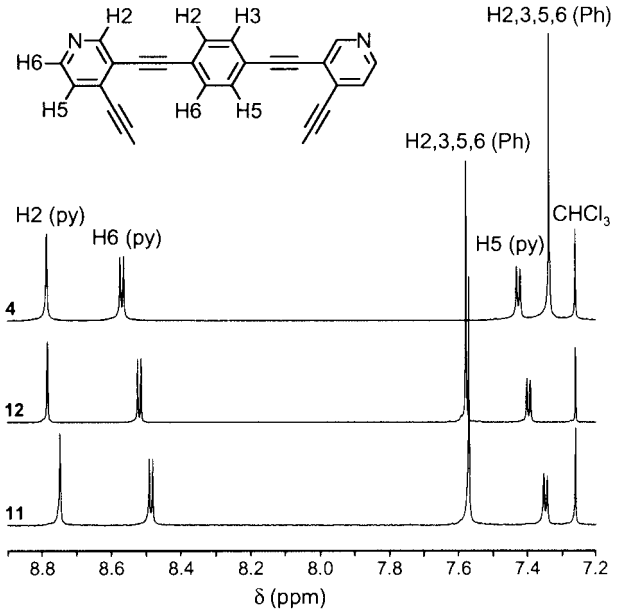

Figure 1. 500 MHz ^{1}H NMR spectra of **4**, **11** and **12** recorded in $CDCl_3$ at 20 °C.

was a helically twisted macrocycle, with the central two phenyl rings lying parallel to each other, and at a mean plane distance of 5.28 Å. The hinged nature of the molecule allows some conformational flexibility and variation in the inter-phenyl distance. The AM1-calculated structure of **4** is in agreement with the crystal structure of the parent hydrocarbon, which also exhibits a helical molecule with a parallel arrangement of the central benzene rings.[15b] However, the distance of 3.68 Å between the two parallel 1,4-phenyl rings in the latter macrocycle is significantly shorter than that of **4**, and presumably results from compression of the molecule induced by crystal packing.[28b]

Twistophane **4** was found to exhibit good solubility in organic solvents such as $CHCl_3$, CH_2Cl_2, and toluene. Solutions of **4** were also rather light sensitive, and rapidly darkened in colour upon exposure to direct light. Gradual heating of **4** up to 300 °C resulted in the formation of an infusible solid with no visual melting behaviour. Surprisingly however, placement of samples in a melting point apparatus operating at temperatures above 257 °C caused the product to ignite explosively, with the concomitant formation of a black soot. In this latter respect, **4** exhibits similar behaviour to a previously reported dehydrotetrabenzoannulene[5] and a family of spiro-linked [*n*]rotanes.[10a, b] The thermal behaviour of **4** is particularly interesting as it suggests that compounds of this type may also afford a route to carbon nanotubes and/or fullerenes.

Metal ion sensing by twistophane 4: To assess the potential utility that twistophane **4** may offer for the sensory detection of metal ions, a detailed spectroscopic investigation into its cation-binding properties was undertaken.

The UV/Vis spectra of uncomplexed **4** in CH_2Cl_2 and 10 % $MeOH/CH_2Cl_2$ solutions exhibit three absorbances at 301, 318 and 362 nm that are invariant in energy and shape over the concentration range of $2.5 \times 10^{-6} - 2.5 \times 10^{-5}$ mol dm^{-3}, showing that aggregation is not occurring in dilute solution.

UV/Vis spectra were then recorded of 1:4 stoichiometric mixtures of **4**: M^{n+} in 10 % $MeOH/CH_2Cl_2$, where $[\mathbf{4}] = 8.58 \times 10^{-6}$ mol dm^{-3} and $M^{n+} = Li^{I}$, Na^{I}, K^{I}, Mg^{II}, Ca^{II}, Cr^{III}, Mn^{II}, Pt^{II}, Au^{I}, Cu^{I}, Cu^{II}, Zn^{II}, Cd^{II}, Pb^{II}, Tl^{I}, Al^{III}, In^{III}, Sc^{III}, Y^{III}, La^{III}, Eu^{III}, Tb^{III}.[29] All spectra showed zero or minimal changes compared to the UV/Vis spectrum of **4**, indicating insignificant binding of the macrocycle to the above cations in dilute solution. However, the UV/Vis spectra of stoichiometric 1:4 combinations of **4**/Hg^{II} and **4**/Pd^{II} in 10 % $MeOH/CH_2Cl_2$, where $[\mathbf{4}] = 8.58 \times 10^{-6}$ mol dm^{-3}, were significantly different from the spectrum of pure **4**, demonstrating that coordination of these ions was occurring. The addition of Hg^{II} ions caused a small but significant reduction in the free-ligand absorbances at 301 and 362 nm, and a broadening of the latter absorption envelope towards longer wavelengths (Figure 3). The presence of Pd^{II} ions on the other hand engendered a large increase in the intensities and a concomitant shift to longer wavelengths of all three free-ligand absorbance envelopes of **4** (Figure 3). In an ion-binding competition study, the UV/Vis spectrum of a 1:4:4 mixture of **4**/Hg^{II}/Pd^{II} in 10 % $MeOH/CH_2Cl_2$ was recorded where $[\mathbf{4}] = 8.58 \times 10^{-6}$ mol dm^{-3}. The spectrum of the mixture showed a much greater similarity to that of the 1:4 **4**/Pd^{II} solution, and with complete extinction of the free ligand fluorescence (see

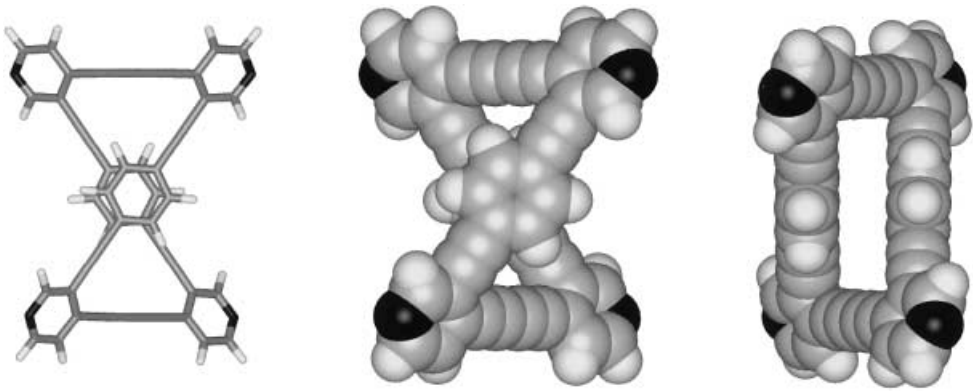

Figure 2. Energy-minimised structure of macrocycle **4**, showing the twisted chiral ground state conformation. Left: plan view (stick representation); centre: plan view (CPK representation); right: view through central macrocyclic cavity. The minimisation was obtained by an AM1 semi-empirical calculation using SPARTAN 02 Linux/Unix, Wavefunction, Inc., Irvine, CA, USA.

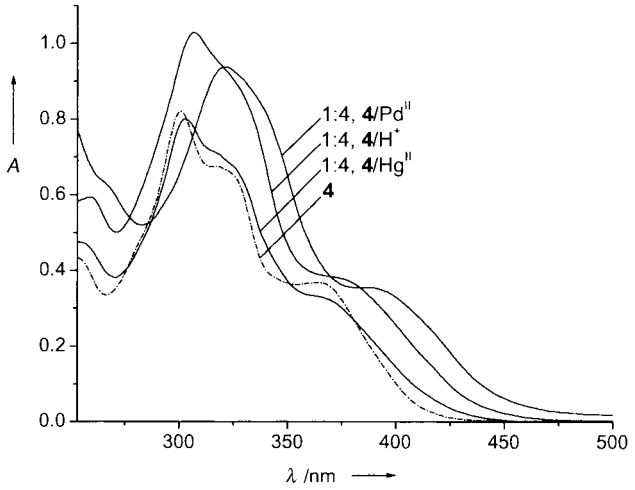

Figure 3. UV/Vis absorption spectra of 1:4, **4**/M^{n+} in 10% MeOH/CH_2Cl_2, where $M^{n+} = Hg^{II}$ and Pd^{II} at a [**4**] of 8.58×10^{-6} mol dm^{-3}.

below), demonstrating that Pd^{II} ions bind more strongly to **4** than Hg^{II} ions.

Interestingly, yellow precipitates developed upon preparation of 1:4 stoichiometric mixtures of **4**/M^{n+} in 10% MeOH/CH_2Cl_2, where $M^{n+} = Fe^{II}$, Co^{II}, Ni^{II} and Ag^{I} and [**4**] $= 8.58 \times 10^{-6}$ mol dm^{-3}. The precipitates formed immediately with Ag^{I} and within 4–15 mins after admixture of **4** with the other three metal ions. A more detailed investigation into the **4**/Ag^{I} system revealed that precipitate formation occurred with **4**/Ag^{I} ratios between 1:2 and 1:3. However, the UV/Vis spectra of solutions with **4**/Ag^{I} ratios of 1:1–1:2 showed no evidence of binding of Ag^{I} to **4**. In the case of Ag^{I}, the binding interaction with **4** must be very weak at low [**4**], yet increasing the relative amount of Ag^{I} beyond the 1:2 **4**/Ag^{I} threshold ratio must result in the generation of minute quantities of highly insoluble coordination oligomers and/or polymers. Once oligomer/polymer precipitation has started, the speciation equilibria presumably continually re-adjust until the bulk of the reactants have passed out of solution. Addition of a few drops of a saturated 10% H_2O/MeOH solution of KCN to the 1:4 **4**/Ag^{I} mixture caused complete disappearance of the precipitate and regeneration of the original UV/Vis spectrum of **4**. This latter observation demonstrated that the suspended solid was a coordination polymer, and not the product of an irreversible chemical reaction.

To assess the effect of interference between mixtures of ions on the binding, and ultimately the potential utility of **4** as a sensor, UV/Vis competition experiments were investigated with 1:4:4 mixtures of **4**/$M1^{2+}$/$M2^{n+}$ in 10% MeOH/CH_2Cl_2, where [**4**] $= 8.58 \times 10^{-6}$ mol dm^{-3}, $M1^{2+} = Pd^{II}$ and Hg^{II}, and $M2^{n+} = Fe^{II}$, Co^{II}, Ni^{II} and Ag^{I}. From these latter studies, the overall ion-binding preference of **4** was found to occur in the following qualitative order, $Pd^{II} > Co^{II} \cong Ni^{II} \cong Ag^{I} > Fe^{II} \cong Hg^{II}$. Thus the presence of Pd^{II} with Fe^{II}, Co^{II}, Ni^{II} and Ag^{I} suppressed precipitation in all four cases, but the **4**/Hg^{II}/$M2^{n+}$ mixtures where $M2^{n+} = Co^{II}$, Ni^{II} and Ag^{I} developed precipitates after 24 h.

The precipitation phenomenon discussed above is particularly noteworthy as it demonstrates that **4** can function as a precipitation sensor for select group of transition-metal ions and chorides, providing Pd^{II} ions and to a lesser extent Hg^{II} ions are absent.[30]

Solutions of **4** in organic solvents emit a purple-blue fluorescence when irradiated with UV light. The fluorescence emission of **4** in aerated and deoxygenated CH_2Cl_2 solution comprised a single broad maximum at 453 nm when excited at the wavelength of the absorption envelope at 301 nm. The excited state of **4** is therefore insensitive to quenching by oxygen. The energy of the emission maximum remained unchanged over the concentration range of 2.45×10^{-7}–2.45×10^{-5} mol dm^{-3}, showing that aggregation of the excited state was also not occurring in dilute solution. Changing the solvent to aerated 10% MeOH/CH_2Cl_2 also had a negligible effect upon the emission spectrum of **4**.

Fluorescence emission spectra of 1:4 solutions of **4**/M^{n+} in 10% MeOH/CH_2Cl_2 were then recorded, where [**4**] $= 2.45 \times 10^{-6}$ mol dm^{-3}, and M^{n+} = all cations and metal chlorides investigated in the UV/Vis spectroscopic studies described above. In the case of Ag^{I}, Fe^{II}, Co^{II}, and Ni^{II}, fluorescence changes were qualitatively observed upon precipitation. The precipitation process within the 1:4 **4**/M^{n+} mixtures, where $M^{n+} = Co^{II}$ and Ni^{II}, was accompanied by a slight visual fluorescence colour change from blue-purple to blue-green. Varying degrees of partial fluorescence quenching also occurred during precipitation in the 1:4 **4**/M^{n+} mixtures, where $M^{n+} = Ag^{I}$, Fe^{II} and Co^{II}. Of all other metals examined, only Hg^{II} and Pd^{II} evoked changes in the solution fluorescence emission of **4**, and in both cases caused quenching of the fluorescence of the macrocycle. The fluorescence quenching is illustrated for the **4**/Pd^{II} system, which shows the spectra of solutions of **4** with incremental additions of Pd^{II} (Figure 4). From this titration experiment, the detection limit for Pd^{II} was

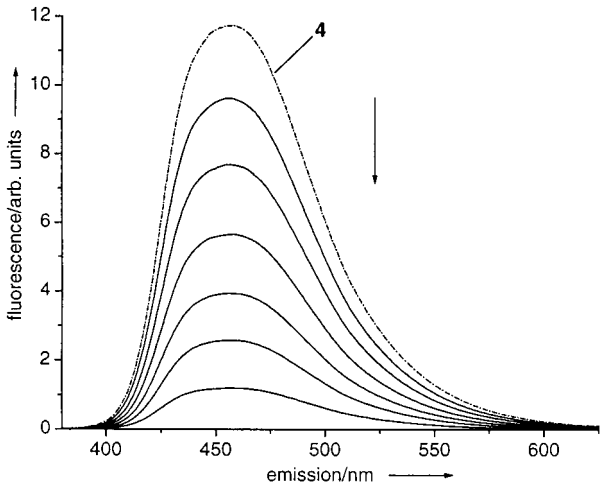

Figure 4. Fluorescence emission spectra of **4** with incremental additions of Pd^{II} at a [**4**] $= 2.45 \times 10^{-6}$ mol dm^{-3} in 10% MeOH/CH_2Cl_2, and **4**/Pd^{II} ratios of respectively 1:0.25, 1:0.5, 1:0.75, 1:1, 1:1.5, and 1:2 (325 nm excitation).

estimated to be at [Pd^{II}] $= 1 \times 10^{-6}$ mol dm^{-3}. A comparable fluorescence quenching titration experiment with **4** and increasing amounts of Hg^{II} in 10% MeOH/CH_2Cl_2 established the detection limit for Hg^{II} to be at [Hg^{II}] $= 9 \times 10^{-6}$ mol dm^{-3}. The above measurements were however hampered by slow,

time-dependent spectral changes, which suggest that the complexation of **4** by Hg^{II} and Pd^{II} each involves the generation of a suite of species, the most kinetically stable of which are formed initially, and which then redistribute over time to the thermodynamically favoured speciation profile.

The latter results demonstrate that cyclophane **4** functions as a particularly selective complexant and ion sensor in solution at high dilution. Of the 24 non-precipitate-forming metal ions and chlorides investigated, only two, that is Hg^{II} and Pd^{II}, produced spectroscopically detectable signals indicative of binding to **4**. The ion-binding preferences of **4** differ markedly from those of the structurally related twistophanes **1**–**3**, in that **4** shows no spectroscopic evidence for coordination to Cu^{II} or Cu^{I} in dilute solution. A bidentate, chelating, nitrogen-donor ligand binding-site appears therefore to be a minimum requirement for coordination to the latter two ions under dilute conditions. This observation suggests that ion sensory systems based on conjugated ethynyl–pyridyl architectures related structurally to **4**, may achieve the difficult task of detecting and distinguishing first row transition metals in cases where Cu^{II}/Cu^{I} interfere.

Proton sensing by twistophane 4: The fluorescence wavelength and intensity of **4** is also sensitive to the presence of protons. In a qualitative investigation of this process, CF_3COOH was titrated into a 2.45×10^{-6} mol dm^{-3} solution of **4** in CH_2Cl_2, and the fluorescence emission spectral changes recorded (Figure 5). At comparatively low acid concentrations, (1×10^{-5}–1×10^{-4} mol dm^{-3}), the colour of the fluorescence emission of **4** remained unaffected. However, a

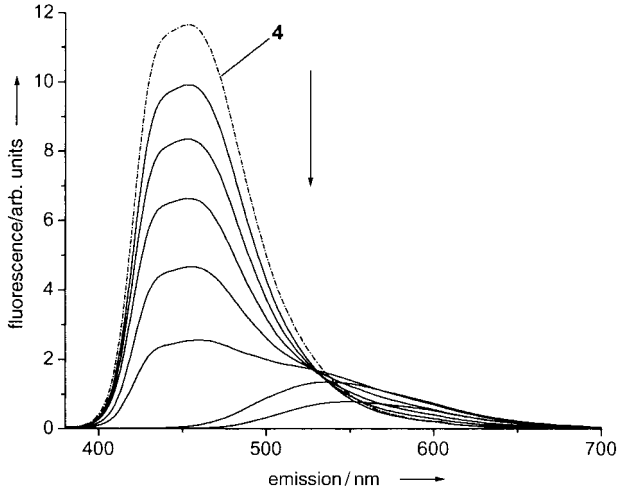

Figure 5. Fluorescence emission spectra of **4** with incremental additions of CF_3COOH at a [**4**] = 2.45×10^{-6} mol dm^{-3} in CH_2Cl_2, and [H^+] of respectively, 1×10^{-5}, 1×10^{-4}, 2.5×10^{-4}, 5×10^{-4}, 1×10^{-3}, 1×10^{-2} and 1×10^{-1} mol dm^{-3} (301 nm excitation).

stepwise increase in the [H^+] from 1×10^{-4} to 1×10^{-1} mol dm^{-3}, resulted in colour changes from pale blue through white, yellow and finally orange, upon visualisation with a UV lamp operating at 365 nm. The fluorescence emission spectra of the **4**/H^+ solutions exhibited strong proton induced quenching in the fluorescence of **4** as the [H^+] was increased, with almost total extinction of the original emission maximum at [H^+] > 0.1 mol dm^{-3}. A longer wavelength, low intensity emission envelope at 550 nm also developed at high [H^+], the growth of which presumably contributed to the observed colour changes described above. Extraction of the solution of **4**, where [H^+] = 0.1 mol dm^{-3}, with aqueous NaOH, caused complete regeneration of the original unprotonated spectrum of the macrocycle. This demonstrates that the CF_3COOH initiated fluorescence changes in **4** were due to reversible acid-base equilibria and not irreversible chemical reactions.

The interesting acid-modulated fluorescence behaviour of **4** arises directly from proton-induced redistributions of electron density within the conjugated macrocyclic framework, relayed through the nitrogen lone pairs. Twistophane **4** may thus be considered to be one of the first members of a structurally new lead class of proton sensory materials.[31a–d]

Metal ion sensing by precursor 11: A comparative spectroscopic investigation into the metal ion binding properties of acyclic precursor **11** was also undertaken to reveal the effect of macrocyclic conjugation on the complexation and sensory abilities of **4**.

The UV/Vis spectra of **11** in CH_2Cl_2 and 10% MeOH/CH_2Cl_2 comprise four bands at 260, 317, 342 and 360 nm. The spectra are invariant in energy and shape at $\leq 4 \times 10^{-5}$ mol dm^{-3}, showing that aggregation is not occurring in dilute solution.

The metal ion binding experiments were conducted using a 1:2 ratio of **11**/M^{n+} in 10% MeOH/CH_2Cl_2 where [**11**] = 1.72×10^{-5} mol dm^{-3}, and M^{n+} = all cations and metal chlorides investigated in the spectroscopic studies of **4** above. In this case, no metal ion induced precipitation phenomena were observed for any **11**/M^{n+} mixture. In addition, the 1:2 **11**/M^{n+} combinations where $M^{n+} = Ag^{I}$, Fe^{II}, Co^{II}, and Ni^{II} showed negligible or zero UV/visible and fluorescence spectroscopic changes. Similarly to **4** however, the UV/Vis spectrum of **11** did undergo significant changes upon addition of Hg^{II} and Pd^{II} indicative of binding to these ions. Specifically, the latter metals caused a sharp increase in intensity and movement to longer wavelength of the 260 nm absorption envelope, and a decrease in intensity and shift to longer wavelength of the 342 and 360 nm absorptions (Figure 6). The UV/Vis spectrum of the 1:2 **11**/Hg^{II} system also underwent gradual, time-dependent changes, presumably originating from a binding mechanism that involves slow kinetics.

Interestingly and somewhat surprisingly, the UV/Vis spectra of 1:2 **11**/M^{n+} mixtures in 10% MeOH/CH_2Cl_2, where $M^{n+} = Al^{III}$, Sc^{III} and In^{III}, exhibited small but significant changes compared to the spectrum of uncomplexed **11** (Figure 7). The presence of these ions caused a slight decrease in intensity of the 260, 342 and 360 nm absorptions of **11**, and the development of a characteristic low intensity longer wavelength shoulder at 388 nm. This evidence suggests that a weak binding interaction exists between **11** and Al^{III}, Sc^{III} and In^{III} in dilute solution.

Solutions of **11** in organic solvents also emit a purple-blue fluorescence when irradiated with UV light. The fluorescence emission spectra of **11** in aerated and deoxygenated CH_2Cl_2 solution are identical when excited at the wavelength of the

absorption envelope at 342 nm, and comprise two emission maxima at 373 and 390 nm. The excited state of **11** is therefore

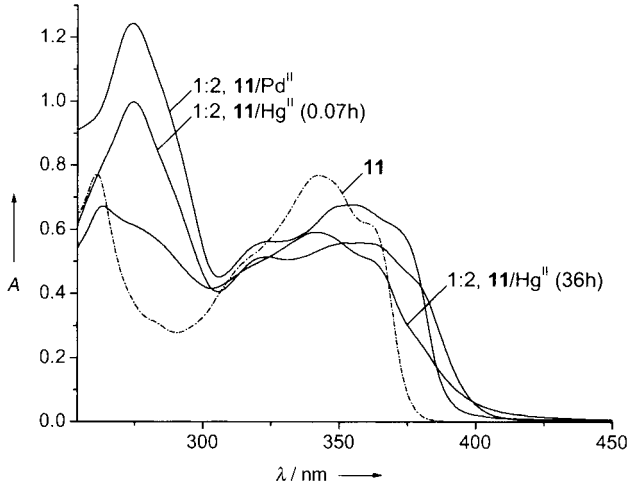

Figure 6. UV/Vis absorption spectra of 1:2 **11**/M^{n+} solutions in 10% $MeOH/CH_2Cl_2$, where $M^{n+} = Hg^{II}$ and Pd^{II} at a [**11**] of 1.72×10^{-5} mol dm^{-3}.

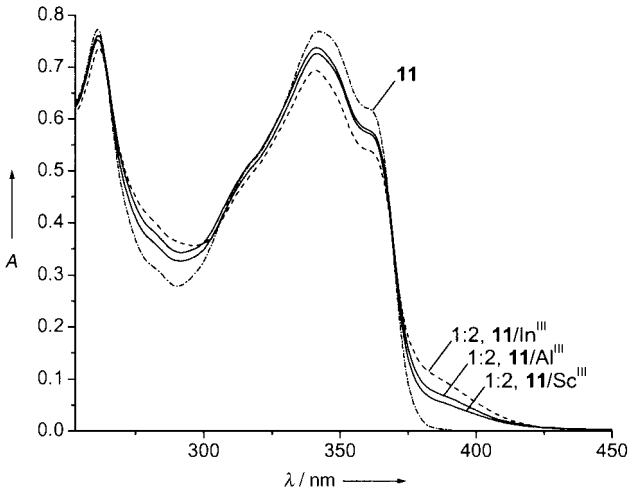

Figure 7. UV/Vis absorption spectra of 1:2 **11**/M^{n+} solutions in 10% $MeOH/CH_2Cl_2$, where $M^{n+} = Al^{III}$, Sc^{III} and In^{III} at a [**11**] of 1.72×10^{-5} mol dm^{-3}.

insensitive to quenching by oxygen. Changing the solvent to aerated 10% $MeOH/CH_2Cl_2$ also had a negligible effect upon the emission spectrum of **11**.

A qualitative investigation into the fluorescence response of **11** towards all the metal ions and chlorides examined in the UV/visible spectroscopic ion binding studies of **11** above, was carried out under identical conditions, at $[\mathbf{11}] = 1.72 \times 10^{-5}$ mol dm^{-3} in 10% $MeOH/CH_2Cl_2$. These investigations revealed visually that the coordinating analytes Hg^{II}, and Pd^{II} caused respectively, partial and complete fluorescence quenching of **11**. The metal ions Al^{III}, Sc^{III} and In^{III} induced small visual colour changes in the fluorescence emission of **11**, that is, from purple-blue to a slightly paler purple-blue. The Cr^{III} ion also caused a slight visual change in the fluorescence emission of **11**. This latter change was of a similar nature to that induced by Al^{III}, Sc^{III} and In^{III} ions, despite the fact that the UV/Vis spectrum of the 1:2 **11**/Cr^{III} system indicated only a negligible binding interaction. All other 1:2 **11**/M^{n+} mixtures studied gave zero coordination-induced fluorescence emission responses.

Thus macrocycle **4** binds six, and **11** binds five out of the twenty eight metal ions and chlorides studied. Both ligands therefore exhibit approximately similar complexation selectivities. The sensory selectivities of **4** and **11** were also quite high and qualitatively similar, as they both only gave strong fluorescence emission output responses in the presence of Hg^{II} and Pd^{II}.

The metal ion binding preferences of **11** are however, surprisingly different from those of **4**, considering the basic structural similarity of the subunits of both ligands. Unlike **4**, acyclic **11** shows negligible or zero coordination affinity towards the transition metal ions Ag^{I}, Fe^{II}, Co^{II}, and Ni^{II}, but does exhibit preferential binding interactions with triply charged ions, that is, Al^{III}, Sc^{III} and In^{III}.[32] The reason why **11** fails to generate coordination polymer precipitates in dilute solution may originate from the fact that it has only two metal ion binding sites, thereby restricting the degree of branching during polymer growth. Macrocycle **4** on the other hand, possesses four ion-binding sites which would be expected to enable rapid branching and access to comparatively high molecular mass structures at an early stage in the coordination polymerisation reaction. In the latter scenario, highly branched, high molecular mass coordination oligomers and polymers would be expected to be of lower solubility, and to precipitate rapidly from solution. Cyclophane **4** is therefore unusual in that it is able to visually signal and distinguish the presence of particular metal ions both by fluorescence and precipitation.[33]

Conclusion

The above work describes the successful preparation of twistophane **4**, which, to the best of the author's knowledge, is the first reported example of a dehydropyridoannulene-type cyclophane with enforced exotopic metal ion-binding sites. The latter molecule thus represents a new type of cyclically conjugated and chiral ligand scaffold capable of coordinating metal ions and complexes to its external surface. Cyclophane **4** was obtained by using an economic and efficient synthesis in relatively few steps, in (19%) overall yield. The characterisation of **4** as a macrocyclic entity was based upon mass spectrometric and IR and NMR spectroscopic evidence, and its twisted, chiral three-dimensional architecture supported by molecular modelling studies.

Owing to the enhanced cyclic conjugation in the absence of chelating coordination sites, it was anticipated that **4** would function as a metal ion sensor, but with completely different ion-binding preferences to those of **1**–**3**. Subsequent spectroscopic investigations confirmed that **4** and acyclic precursor **11** did indeed function as metal ion sensors. Both ligands were found to be particularly selective sensors, giving fluorescence quenching output responses for only two of all the metal ions and chlorides studied, that is Hg^{II} and Pd^{II}.[34] Ligands **4** and **11** therefore represent a new structural design principle for the

future creation of fluorescence sensors of specific heavy metal toxins and pollutants, a result of especial interest in relation to environmental issues.[35a–c] Also of particular note, is the dual ion-sensory output ability of **4**, which can signal the presence of different metals by fluorescence or precipitation.

The precipitates are almost certainly coordination polymers of **4**, which may be branched and dendritic in nature and/or crosslinked networks. The latter possibility is very interesting, as three-dimensional coordination networks comprising **4** and specific first-row transition-metal ions may exhibit a range of fascinating bulk electronic and magnetic properties.[36a–e] Such properties may be anticipated due to the conjugated nature of bridging **4** ligands, which should enable facile electronic communication between the metal ions in all dimensions throughout the polymer network.

Interestingly, **4** also functions as a proton-triggered fluorescence sensor, a finding that suggests that **4** and structurally related compounds may discover applications in the field of molecular protonics. Lastly, **4** was found to function as a high-energy material, explosively igniting above a particular temperature threshold upon rapid heating.

Twistophane **4** thus represents a structurally unique conjugated ligand which is able to act both as a selective fluorescence and precipitation sensor for particular metal ions. The fascinating metal coordination properties of this macrocycle suggest that **4** and related structures will discover many future applications in the fields of ionic and molecular sensorics,[37] crystal engineering,[38a–e] materials science[39a–e] and in the design and construction of metal-assembled nanoarchitectures.[40a–c]

Experimental Section

General: Standard inert atmosphere and Schlenk techniques were employed for reactions conducted under argon. The THF used in the lithiation/iodination of **5** and **7** was dried by distillation off sodium/benzophenone under argon. Starting materials **5**, **9**, and catalysts $[PdCl_2(PPh_3)_2]$[41] and CuI were purchased from Aldrich, and the $[Cu_2(OAc)_4]$ was purchased from Prolabo and used as received. The triethylamine and THF used in the preparation of **7** and **11** were deoxygenated by bubbling with argon for 0.5 h directly prior to use. The alumina used for the chromatographic purification of macrocycle **4** was purchased from Merck (Aluminium Oxide, Basic, activity I) and converted to activity IV upon prolonged mixing with distilled water for 8 h prior to use. The silica used for all flash chromatography was also purchased from Merck (Geduran, Silica gel Si 60, 40–63 μm).

Intramolecular proton connectivities were determined by $^1H-^1H$ COSY and NOESY NMR measurements where necessary. All ^1H and ^{13}C NMR spectra were referenced to the solvent peaks (at 7.26 and 77.0 ppm, respectively). The fluorescence emission spectra were recorded at 20–25 °C on a Aminco, Bowman Series 2 luminescence spectrophotometer (SLM Instruments, Inc.). The free ligand fluorescence emission spectra of **4**, **11** and **12** given below were recorded in argon bubbled CH_2Cl_2 and were corrected for the instrumental response. The fluorescence emission spectra of the metal ion binding experiments with **4** and **11** were conducted in aerated 10% MeOH/CH_2Cl_2, to obtain optical responses under environmental conditions of most practical utility for sensory applications. The infrared spectrum of **4** was recorded as nujol and polychlorotrifluoroethylene mulls, all other IR spectra were recorded as compressed KBr discs. Melting point measurements were performed on an Electrothermal Digital Melting Point apparatus calibrated with standards of known melting points. Elemental analyses were performed by the Service de Microanalyse, Institut de Chimie, Université Louis Pasteur.

3-Bromo-4-iodopyridine (6): THF (250 mL) which had been freshly distilled off Na/benzophenone under argon, was added by syringe to a dried, argon-filled, 500-mL two-necked round-bottomed flask equipped with a vacuum/argon inlet adaptor, alcohol thermometer, rubber septum and a large magnetic stirrer ovoid. The stirred THF was then cooled to an internal temperature of −78 °C using a liquid N_2/CO_2/hexane bath. Diisopropylamine (12 mL, 8.604 g, 8.503×10^{-2} mol) was then added by syringe, and after a further 5 min stirring, *n*-butyllithium (1.6 M in hexanes; 60 mL, 0.096 mol) was syringed into the solution at a rate which maintained the internal temperature at between −78 and −70 °C. The resulting LDA solution was stirred at −78 °C for 0.5 h to allow for completion of the reaction, and subsequently cooled to −85 °C. Neat **5** (15 g, 9.494×10^{-2} mol) was then syringed into the stirred LDA solution at a rate which maintained the internal temperature between −85 and −80 °C. The resulting yellow solution was re-cooled to −85 °C and stirred at this temperature for 0.75 h, during which time it became deep maroon in colour. The stirred reaction was subsequently allowed to warm to −75 °C for 10 min, then re-cooled to −85 °C and stirred at this temperature for 0.5 h. THF (40 mL) was syringed into a dried, argon-filled schlenk containing iodine (25 g, 0.197 mol), and the mixture stirred until all the iodine had dissolved. The iodine solution was then added dropwise by syringe to the lithiopyridine reaction mixture at a rate which maintained the internal temperature between −85 and −75 °C. By the end of the addition, the reaction had become dark brown in colour. The mixture was stirred at −78 °C for a further 4 h, then allowed to warm to ambient temperature with continued stirring overnight. Distilled water (10 mL) was added to quench the reaction and the solvent volume reduced to approximately 75 mL by distillation under reduced pressure on a water-bath. The remaining dark mixture was then partitioned between Et_2O and excess saturated $Na_2S_2O_3$, and subsequently extracted repeatedly with Et_2O (5×200 mL) due to the poor solubility of the suspended **6**. The combined organic extracts were dried (anhydrous $MgSO_4$), gravity filtered, and the solvent removed by distillation on a waterbath at atmospheric pressure. The remaining pale-brown solid was chromatographed three times on a large column of silica, eluting with CH_2Cl_2, to yield **6** (16.8g, 69%) as a dusty cream microcrystalline solid. M.p. 111.8–112.8 °C, recrystallisation from EtOH; (M.p. 112 °C).[22b]

^1H NMR ($CDCl_3$, 500 MHz, 27 °C): $\delta = 8.694$ (s, 1H; H2), 8.116 (d, $^3J(6,5) = 5.1$ Hz, 1H; H6), 7.814 ppm (d, $^3J(5,6) = 5.1$ Hz, 1H; H5); ^{13}C NMR ($CDCl_3$, 125.8 MHz, 27 °C): $\delta = 150.9$, 147.6, 135.1, 128.9, 112.2 ppm; IR: $\tilde{\nu} = 3032$ (w), 1554 (s), 1541 (s), 1447 (s), 1388 (s), 1266 (s), 1174 (s), 1113 (s), 1058 (s), 1016 (s), 1008 (s), 821 (s), 707 (s), 656 (s), 508 (s), 412 cm^{-1} (s); FABMS ($CHCl_3$): *m*/*z* (%): 283.9 (100) $[M^+ + H]$; HRMS (FAB, $CHCl_3$, $[M^+ + H]$) calcd. for C_5H_4BrIN: 283.8572; found: 283.8584.

3-Bromo-4-(trimethylsilylethynyl)pyridine (7): Et_3N (72 mL), which had been bubbled with argon, was added by syringe to a mixture of **6** (5.03 g, 1.772×10^{-2} mol) and $[PdCl_2(PPh_3)_2]$ (0.130g, 1.852×10^{-4} mol) under an atmosphere of argon. The mixture was stirred until all the **6** had dissolved, and then trimethylsilylacetylene (1.946 g, 1.981×10^{-2} mol) and a solution of CuI (0.116 g, 6.091×10^{-4} mol) in degassed Et_3N (6 mL) added consecutively by syringe. The reaction was stirred for seven days at ambient temperature in the dark, during which time a finely divided brown suspension formed. All solvent was then distilled off under reduced pressure on a water bath at 80 °C, and CH_2Cl_2 (30 mL) was added. The mixture was subsequently flash-chromatographed on a column of silica, eluting with CH_2Cl_2. A dark brown band eluted first which was closely followed by **7**. The product thus obtained was dried under vacuum to give **7** (4.091 g, 91%) as a pale off-yellow oil.

^1H NMR ($CDCl_3$, 500 MHz, 27 °C): $\delta = 8.742$ (s, 1H; H2), 8.453 (d, $^3J(6,5) = 4.9$ Hz, 1H; H6), 7.331 (dd, $^3J(5,6) = 4.9$ Hz, $^5J(5,2) = 0.5$ Hz, 1H; H5), 0.290 ppm (s, 9H; $Si(CH_3)_3$); ^{13}C NMR ($CDCl_3$, 125.8 MHz, 27 °C): $\delta = 151.7$, 147.7, 132.8, 126.9, 123.2, 105.6 (−C≡), 100.2 (−C≡), −0.44 ppm ($Si(CH_3)_3$); IR: $\tilde{\nu} = 2960$ (m), 2169 (w) (C≡C), 1574 (s), 1466 (m), 1396 (m), 1251 (s), 1086 (m), 1022 (m), 864 (s), 845 (s), 761 (m), 702 cm^{-1} (m); EIMS: *m*/*z* (%): 255 (15) $[M^+]$, 238 (100) $[M^+ - CH_3]$, 173 (18) $[M^+ - HBr]$, 158 (44) $[M^+ - CH_3 - HBr]$; HRMS (FAB, $CHCl_3$, $[M^+ + H]$) calcd. for $C_{10}H_{13}BrNSi$: 254.0001; found: 254.0006.

3-Iodo-4-(trimethylsilylethynyl)pyridine (8): A dried 500-mL two-necked round-bottomed flask charged with **7** (4.043g, 1.590×10^{-2} mol), was equipped with a vacuum/argon inlet adaptor, alcohol thermometer, rubber septum and a magnetic stirrer ovoid. The flask was then evacuated and

back-filled with argon four times in succession and Et_2O (180 mL), which had been freshly distilled off Na/benzophenone under argon, was added by syringe. The stirred solution was subsequently cooled to an internal temperature of $-78\,^{\circ}C$ using a CO_2/acetone bath. A 1.6 M solution of *n*-butyllithium in hexanes (12 mL, 1.920×10^{-2} mol) was added dropwise by syringe at a rate which maintained the reaction temperature between -78 and $-70\,^{\circ}C$. During addition, the initial red colouration of the reaction rapidly discharged to give, finally, a clear pale brown-yellow solution. The reaction solution was then stirred at $-78\,^{\circ}C$ for 1 h. Et_2O (45 mL) was syringed into a dried, argon filled schlenk containing diiodoethane (6.70 g, 2.377×10^{-2} mol), and the mixture stirred until all the diiodoethane had dissolved. The diiodoethane solution was then added dropwise by syringe to the lithiopyridine reaction mixture at a rate which maintained the internal temperature between -78 and $-70\,^{\circ}C$. The reaction was stirred at $-78\,^{\circ}C$ for a further 2.5 h, during which time a copious cream coloured suspension formed, and was then allowed to warm to ambient temperature with continued stirring overnight. The resulting pale yellow solution was extracted with distilled water (3×180 mL), and the organic layer separated, dried (anhydrous $MgSO_4$), filtered, and the Et_2O removed by distillation under reduced pressure at ambient temperature. The remaining dark brown oil was flash chromatographed on a short column of silica, eluting with CH_2Cl_2. Unreacted diiodoethane and some iodine eluted first, eventually followed by **8** which was collected in 350 mL fractions. The product **8** is heat sensitive, and the CH_2Cl_2 is best removed from the column eluates by distillation on a water bath at $\leq 40\,^{\circ}C$ under reduced pressure. Final purification was achieved upon stirring the product **8** with NORIT A decolourising charcoal (0.15 g) in pentane (15 mL), filtering the mixture under gravity, and removal of the solvent by distillation under reduced pressure at ambient temperature. The product was finally dried under vacuum (0.01 mmHg) to yield **8** (4.121 g, 86 %) as a pale yellow-brown oil. The product **8** should be stored at below $-20\,^{\circ}C$ to avoid slow decomposition to a black solid.

^1H NMR ($CDCl_3$, 500 MHz, 25 °C): $\delta = 8.947$ (s, 1H; H2), 8.464 (d, $^3J(6,5) = 4.9$ Hz, 1H; H6), 7.321 (d, $^3J(5,6) = 4.9$ Hz, 1H; H5), 0.298 ppm (s, 9H; $Si(CH_3)_3$); ^{13}C NMR ($CDCl_3$, 125.8 MHz, 25 °C): $\delta = 157.0$, 148.3, 137.1, 126.5, 104.7, 103.6, 99.6 (−C≡), −0.45 ppm ($Si(CH_3)_3$); IR: $\tilde{\nu} = 2959$ (m), 2166 (w) (C≡C), 1567 (s), 1460 (m), 1394 (m), 1274 (m), 1250 (s), 1080 (m), 1011 (m), 865 (s), 845(s), 761 cm^{-1} (m); EIS ($CHCl_3$): *m*/*z* (%): 301 (40) [M^+], 286 (100) [$M^+ - CH_3$], 174 (17) [$M^+ - I$], 158 (19) [$M^+ - CH_3 - HI$]; HRMS (FAB, $CHCl_3$, [$M^+ + H$]) calcd. for $C_{10}H_{13}INSi$: 301.9862; found: 301.9875.

[Benzene-1,4-Bis(2,1-ethynedyil)]bis[3-(4-trimethylsilylethynylpyridine)] (11): THF (25 mL), which had been freshly distilled off Na/benzophenone under argon, was added by syringe to a mixture of **8** (0.803 g, 2.666×10^{-3} mol), **10** (0.158 g, 1.252×10^{-3} mol) and [$PdCl_2(PPh_3)_2$] (0.048 g, 6.839×10^{-5} mol) under an atmosphere of argon. A solution of CuI (0.035 g, 1.838×10^{-4} mol) in Et_3N (3 mL) was then added by syringe, and the mixture stirred at ambient temperature for seven days in the absence of light. During stirring, an orange-brown suspension slowly formed. All solvent was subsequently removed under reduced pressure on a water bath and CH_2Cl_2 (20 mL) was added. The mixture was then chromatographed on a column of alumina (Merck, Aluminium Oxide 90, standardised activity II/III), eluting with CH_2Cl_2. The product **11** co-eluted with a contaminant possessing a slightly higher R_f. The contaminant could however be removed upon first washing the isolated solid product with MeCN, followed by boiling in acetone (15 mL), leaving to cool to ambient temperature, filtering the mixture under vacuum and washing the collected solid with acetone. Final purification was achieved by dissolving the product in boiling acetone (200 mL), gravity filtering the solution and reducing the volume of the filtrate to about 15 mL by distillation on a water bath at atmospheric pressure. After the mixture had been left to stand overnight, it was filtered under vacuum and the collected solid was washed with ice cold acetone and air-dried to yield **11** (0.332 g, 56 %) as a cream-coloured microcrystalline solid. M.p. 197.0–198.1 °C;

^1H NMR ($CDCl_3$, 500 MHz, 25 °C): $\delta = 8.747$ (d, $^5J(2,5) = 0.7$ Hz, 2H; pyridine H2), 8.485 (d, $^3J(6,5) = 5.2$ Hz, 2H; pyridine H6), 7.569 (s, 4H; phenyl H2,3,5,6), 7.347 (dd, $^3J(5,6) = 5.2$ Hz, $^5J(5,2) = 0.7$ Hz, 2H; pyridine H5), 0.292 ppm (s, 18H; $Si(CH_3)_3$); ^{13}C NMR ($CDCl_3$, 125.8 MHz, 25 °C): $\delta = 152.2$, 148.2, 133.0, 131.7, 125.3, 123.1, 121.8, 104.6 (−C≡), 100.6 (−C≡), 95.8 (−C≡), 87.3 (−C≡), −0.28 ppm ($Si(CH_3)_3$); UV/Vis (CH_2Cl_2): λ_{max} (ε) = 260 (52399), 317 (35093), 342 (52179), 360 (41073 $M^{-1}cm^{-1}$); fluorescence emission ([**11**] = 2.71×10^{-6} mol dm^{-3} in CH_2Cl_2, 342 nm excitation): $\lambda_{max} = 373$, 390 nm; IR: $\tilde{\nu} = 2960$ (s), 2221 (m) (C≡C), 2164 (m) (C≡C), 1576 (s), 1510 (s), 1400 (s), 1249 (s), 873 (s), 851 (s), 835 (s), 768 (s), 762 (s), 584 cm^{-1} (s); EIS ($CHCl_3$): *m*/*z* (%): 472 (100) [M^+], 457 (18) [$M^+ - CH_3$], 400 (5) [$M^+ - Si(CH_3)_3$]; elemental analysis calcd (%) for $C_{30}H_{28}N_2Si_2$: C 76.22, H 5.97, N 5.93; found: C 76.04, H 5.58, N 5.80.

[Benzene-1,4-Bis(2,1-ethynedyil)]bis[3-(4-ethynylpyridine)] (12): TBAF (1.8 mL, 1.0 M solution in THF) was added to a stirred solution of **11** (0.332 g, 7.023×10^{-4} mol) in THF (40 mL) and distilled water (0.5 mL). The clear reaction was then stirred at ambient temperature in the absence of light for 20 h. All solvent was removed under reduced pressure on a water bath at 30–40 °C. The remaining solid was dissolved in CH_2Cl_2 (60 mL) and extracted with distilled water (4×30 mL). The organic layer was separated, dried (anhydrous $MgSO_4$) and filtered, and the solvent volume reduced to 15 mL by distillation at atmospheric pressure on a water bath. The concentrate was then chromatographed on a column of alumina (Merck, Aluminium Oxide 90, standardised activity II/III), eluting with CH_2Cl_2. The product thus obtained was finally purified by brief ultrasonication in MeOH (3 mL), filtering under vacuum, and washing the collected solid with MeOH, followed by air drying to give **12** (0.203g, 88 %) as a cream-coloured microcrystalline solid. M.p. 195.0–196.1 °C (decomp; pure by ^1H and ^{13}C NMR spectroscopy).

^1H NMR ($CDCl_3$, 500 MHz, 25 °C): $\delta = 8.784$ (d, $^5J(2,5) = 0.5$ Hz, 2H; pyridine H2), 8.519 (d, $^3J(6,5) = 5.2$ Hz, 2H; pyridine H6), 7.578 (s, 4H; phenyl H2,3,5,6), 7.396 (dd, $^3J(5,6) = 5.2$ Hz, $^5J(5,2) = 0.5$ Hz, 2H; pyridine H5), 3.595 ppm (s, 2H; H−C≡C); ^{13}C NMR ($CDCl_3$, 125.8 MHz, 25 °C): $\delta = 152.4$, 148.3, 132.1, 131.8, 125.8, 123.0, 122.1, 95.9 (−C≡), 86.8 (−C≡), 85.8 (−C≡), 79.7 ppm (−C≡); UV/Vis (CH_2Cl_2): λ_{max} (ε) = 313 (sh) (33893), 338 (51955), 357 (41453 $M^{-1}cm^{-1}$); fluorescence emission ([**12**] = 3.17×10^{-6} mol dm^{-3} in CH_2Cl_2, 338 nm excitation): $\lambda_{max} = 367$, 385 nm; IR: $\tilde{\nu} =$ 3140 (s) (H−C≡), 2222 (m) (C≡C), 2097 (s) (C≡C), 1581 (s), 1528 (s), 1512 (s), 1471 (s), 1402 (s), 833 (s), 757 (s), 581 (s), 353 cm^{-1} (s); FABMS: ($CHCl_3$): *m*/*z* (%): 329 (100) [$M^+ + H$]; HRMS (FAB, $CHCl_3$, [$M^+ + H$]) calcd for $C_{24}H_{13}N_2$: 329.1079; found: 329.1074. The above deprotection reaction was repeated using **11** (0.040 g). After removal of the THF, distilled water (8 mL) was added to the residue and the resulting suspension filtered under vacuum. The portion of compound **12** collected was washed consecutively with a relatively large volume of distilled water (100 mL) and methanol (3 mL), and finally air-dried. This material afforded a satisfactory elemental analysis: elemental analysis calcd (%) for $C_{24}H_{12}N_2$: C 87.79, H 3.68, N 8.53; found: C 87.53, H 3.30, N 8.68.

Macrocycle 4: In a well-ventilated hood, [$Cu_2(OAc)_4$] (2.40g, 6.607×10^{-3} mol) was dissolved in warm pyridine (600 mL), and the stirred solution bubbled with argon for 1.5 h, during which time it cooled to ambient temperature. A solution of **12** (0.183 g, 5.573×10^{-4} mol) in pyridine (20 mL) was then slowly added dropwise over 5 h to the [$Cu_2(OAc)_4$] solution, with continued stirring and argon bubbling. After the addition of **12** was complete, the reaction mixture was stirred under a static atmosphere of argon, at ambient temperature and in the absence of light for 14 days. During the addition of **12**, the reaction mixture changed colour from blue to olive-green, and finally, the development of a red suspended solid was complete after 48 h stirring. All solvent was removed under reduced pressure on a water bath, and pyridine (5 mL) was re-added to wet the residue. An ice-cold concentrated aqueous solution of KCN (30 mL) was then added and the mixture rapidly stirred for 1 h, filtered under vacuum, and the collected solid washed with excess distilled water and air-dried. The dark brown solid was added to CH_2Cl_2 (25 mL) and the cloudy solution chromatographed on a column of alumina (basic, activity IV), eluting with CH_2Cl_2. Due to the enhanced photosensitivity of solutions of **4**, the chromatography and subsequent manipulations are best conducted with shielding from direct light. The product thus obtained was finally briefly ultrasonicated in acetone, filtered under vacuum, and the collected solid washed with excess acetone and air-dried to give **4** (0.130 g, 71 %) as a bright yellow powder. M.p. Slow heating induces colour darkening at $\geq 245\,^{\circ}C$ to give a dark brown infusible solid. Upon rapid heating, **4** ignites explosively at $\geq 257\,^{\circ}C$.

^1H NMR ($CDCl_3$, 500 MHz, 20 °C): $\delta = 8.786$ (s, 4H; pyridine H2), 8.569 (d, $^3J(6,5) = 5.2$ Hz, 4H; pyridine H6), 7.425 (dd, $^3J(5,6) = 5.1$ Hz, $^5J(5,2) =$ 0.7 Hz, 4H; pyridine H5), 7.336 ppm (s, 8H; phenyl H2,3,5,6); ^{13}C NMR ($CDCl_3$, 125.8 MHz, 20 °C): $\delta = 152.0$, 148.4, 131.7, 131.5, 125.0, 123.2, 122.5, 97.3 (−C≡), 86.4 (−C≡), 81.1 (−C≡), 80.3 ppm (−C≡); UV/Vis (CH_2Cl_2): λ_{max}

(ε) = 301 (104611), 318 (84648), 362 (47160 $M^{-1}cm^{-1}$); fluorescence emission ([**4**] = 2.45×10^{-6} mol dm^{-3} in CH_2Cl_2, 301 nm excitation): λ_{max} = 453 nm; IR: $\tilde{\nu}$ = 2210 (s) (C≡C), 2154 (w) (C≡C), 1571 (s), 1526 (m), 1510 (m), 1468 (m), 1405 (s), 837 (s), 826 (s), 762 (m), 578 cm^{-1} (s); FABMS (recorded in 10% $CF_3COOH/CHCl_3$): *m/z* (%): 653 (100) [M^+ + H]; HRMS (FAB, 10% $CF_3COOH/CHCl_3$, [M^+ + H]) calcd for $C_{48}H_{21}N_4$: 653.1766; found: 653.1753.

Acknowledgement

The Collège de France is acknowledged for financial support and Roland Graff for the ^{1}H NMR COSY, NOESY, and ROESY experiments. Dr Bernard Dietrich, Prof. Alexandre Varnek and Dr Jonathan Nitschke are also thanked for helpful discussions.

[1] For an informative series of reviews covering the field up to 1999, see: *Top. Curr. Chem.* **1999**, *201*, whole volume.

[2] a) P. Ruggli, *Justus Liebigs Ann. Chem.* **1916**, *412*, 1; b) P. Ruggli, *Justus Liebigs Ann. Chem.* **1913**, *399*, 174; c) P. Ruggli, *Justus Liebigs Ann. Chem.* **1912**, *392*, 92.

[3] *Top. Curr. Chem.* **1999**, *199*, whole volume.

[4] a) Y. Tobe, H. Nakanishi, M. Sonoda, T. Wakabayashi, Y. Achiba, *Chem. Commun.* **1999**, 1625; b) Y. Tobe, N. Nakagawa, K. Naemura, T. Wakabayashi, T. Shida, Y. Achiba, *J. Am. Chem. Soc.* **1998**, *120*, 4544; c) Y. Rubin, T. C. Parker, S. J. Pastor, S. Jalisatgi, C. Boulle, C. L. Wilkins, *Angew. Chem.* **1998**, *110*, 1353; *Angew. Chem. Int. Ed.* **1998**, *37*, 1226; d) Y. Rubin, *Chem. Eur. J.* **1997**, *3*, 1009, and references therein.

[5] R. Boese, A. J. Matzger, K. P. C. Vollhardt, *J. Am. Chem. Soc.* **1997**, *119*, 2052.

[6] a) U. H. F. Bunz, Y. Rubin, Y. Tobe, *Chem. Soc. Rev.* **1999**, *28*, 107; b) F. Diederich, *Nature* **1994**, *369*, 199; c) U. H. F. Bunz, *Angew. Chem.* **1994**, *106*, 1127; *Angew. Chem. Int. Ed. Engl.* **1994**, *33*, 1073; d) F. Diederich, Y. Rubin, *Angew. Chem.* **1992**, *104*, 1123; *Angew. Chem. Int. Ed. Engl.* **1992**, *31*, 1101.

[7] a) E. Mena-Osteritz, P. Bäuerle, *Adv. Mater.* **2001**, *13*, 243; b) J. S. Moore, *Acc. Chem. Res.* **1997**, *30*, 402.

[8] a) S. Eisler, R. R. Tykwinski, *Angew. Chem.* **1999**, *111*, 2138; *Angew. Chem. Int. Ed. Engl.* **1999**, *38*, 1940; b) A. M. Boldi, F. Diederich, *Angew. Chem.* **1994**, *106*, 482; *Angew. Chem. Int. Ed. Engl.* **1994**, *33*, 468.

[9] a) L. T. Scott, M. J. Cooney, C. Otte, C. Puls, T. Haumann, R. Boese, P. J. Carroll, A. B. Smith III, A. de Meijere, *J. Am. Chem. Soc.* **1994**, *116*, 10275; b) L. T. Scott, G. J. DeCicco, J. L. Hyun, G. Reinhardt, *J. Am. Chem. Soc.* **1985**, *107*, 6546. It may be noted that the name "pericyclynes" used in the latter two references has been replaced by the name "pericyclines" in the review of reference [1].

[10] a) A. de Meijere, S. Kozhushkov, T. Haumann, R. Boese, C. Puls, M. J. Cooney, L. T. Scott, *Chem. Eur. J.* **1995**, *1*, 124; b) A. de Meijere, S. Kozhushkov, C. Puls, T. Haumann, R. Boese, M. J. Cooney, L. T. Scott, *Angew. Chem.* **1994**, *106*, 934; *Angew. Chem. Int. Ed. Engl.* **1994**, *33*, 869.

[11] a) R. H. Mitchell, *Isr. J. Chem.* **1980**, *20*, 294; b) P. J. Garratt in *Comprehensive Organic Chemistry; The Synthesis and Reactions of Organic Compounds*, *Vol. 1* (Ed.: J. F. Stoddart), Pergamon, Oxford, **1979**, Chapter 2.6, p. 361; c) H. Meier, *Synthsis* **1972**, 235.

[12] a) J. M. Kehoe, J. H. Kiley, J. J. English, C. A. Johnson, R. C. Petersen, M. M. Haley, *Org. Lett.* **2000**, *2*, 969; b) W. J. Youngs, C. A. Tessier, J. D. Bradshaw, *Chem. Rev.* **1999**, *99*, 3153; c) J. J. Pak, T. J. R. Weakley, M. M. Haley, *J. Am. Chem. Soc.* **1999**, *121*, 8182; d) M. M. Haley, *Synlett* **1998**, 557.

[13] a) K. Campbell, C. J. Kuehl, M. J. Ferguson, P. J. Stang, R. R. Tykwinski, *J. Am. Chem. Soc.* **2002**, *124*, 7266; b) D. Venkataraman, S. Lee, J. Zhang, J. S. Moore, *Nature* **1994**, *371*, 591.

[14] J. Zhang, J. S. Moore, *J. Am. Chem. Soc.* **1994**, *116*, 2655.

[15] For the syntheses of dehydrotetrabenzoannulenes and related structures, see: a) M. L. Bell, R. C. Chiechi, C. A. Johnson, D. B. Kimball, A. J. Matzger, W. Brad Wan, T. J. R. Weakley, M. M. Haley, *Tetrahedron* **2001**, *57*, 3507; b) S. K. Collins, G. P. A. Yap, A. G. Fallis, *Org. Lett.* **2000**, *2*, 3189; c) S. K. Collins, G. P. A. Yap, A. G. Fallis, *Angew. Chem.* **2000**, *112*, 393; *Angew. Chem. Int. Ed.* **2000**, *39*, 385; d) M. M. Haley, M. L. Bell, J. J. English, C. A. Johnson, T. J. R. Weakley, *J. Am. Chem. Soc.* **1997**, *119*, 2956; e) K. P. Baldwin, R. S. Simons, J. Rose, P. Zimmerman, D. M. Hercules, C. A. Tessier, W. J. Youngs, *J. Chem. Soc. Chem. Commun.* **1994**, 1257. f) See reference [12b]. For the syntheses of dehydrotetrathiophenoannulene-type cyclophanes, see: g) M. J. Marsella, Z.-Q. Wang, R. J. Reid, K. Yoon, *Org. Lett.* **2001**, *3*, 885.

[16] a) P. N. W. Baxter, *Chem. Eur. J.* **2002**, *8*, 5250; b) P. N. W. Baxter, *J. Org. Chem.* **2001**, *66*, 4170.

[17] For examples of ethynyl macrocycles that externally bind metal ions, see; a) O. Henze, D. Lentz, A. Schäfer, P. Franke, A. D. Schlüter, *Chem. Eur. J.* **2002**, *8*, 357. b) See reference [13a]; c) R. Gibe, J. R. Green, *Chem. Commun.* **2002**, 1550; d) M. Laskoski, W. Steffen, J. G. M. Morton, M. D. Smith, U. H, F. Bunz, *Angew. Chem.* **2002**, *114*, 2484; *Angew. Chem. Int. Ed.* **2002**, *41*, 2378; e) K. Campbell, R. McDonald, N. R. Branda, R. R. Tykwinski, *Org. Lett.* **2001**, *3*, 1045. f) See reference [12b].

[18] Pyridine-type ligands connected to/or within electronically delocalised organic scaffolds have been infrequently used for the sensing of metal ions. See for example: a) references [16a-b]; b) P. N. W. Baxter, *J. Org. Chem.* **2000**, *65*, 1257; c) D. T. McQuade, A. E. Pullen, T. M. Swager, *Chem. Rev.* **2000**, *100*, 2537; d) C.-S. Choi, T. Mutai, S. Arita, K. Araki, *J. Chem. Soc. Perkin Trans. 2* **2000**, 243; e) M. Kimura, T. Horai, K. Hanabusa, H. Shirai, *Adv. Mater.* **1998**, *10*, 459; f) B. Wang, M. R. Wasielewski, *J. Am. Chem. Soc.* **1997**, *119*, 12.

[19] The term "twistophane" is used to describe ethynyl cyclophanes that are completely ortho-conjugated, yet helically twisted and therefore non-planar chiral structures. Cyclic organic scaffolds satisfying the latter criteria comprise dehydrotetraarylannulenes, dehydrotetraarylannulene-type cyclophanes and higher homologues. Such materials constitute a small but slowly emergent subclass of conjugated ethynyl macrocycles of which **1**–**4** are the first reported examples with integrated heterocyclic N-donor sites for metal ion coordination.

[20] The thermal-cyclisation reactions of *ortho*-diethynyl pyridines have been the subject of investigation, but reports on the synthesis of such materials remain rare. See: a) C.-S. Kim, K. C. Russell, *J. Org. Chem.* **1998**, *63*, 8229; b) K. J. Gibson, M. d'Alarcao, N. J. Leonard, *J. Org. Chem.* **1985**, *50*, 2462.

[21] Ester and amidic macrocycles and macrobicycles incorporating pyridine rings with outwardly pointing nitrogens, have been the subject of frequent study in the past. For example, as potential NAD^+ and NADH-type macrocyclic catalysts, see: a) Y. Kuroda, H. Seshimo, T. Kondo, M. Shiba, H. Ogoshi, *Tetrahedron Lett.* **1997**, *38*, 3939; b) A. G. Talma, P. Jouin, J. G. De Vries, C. B. Troostwijk, G. H. Werumeus Buning, J. K. Waninge, J. Visscher, R. M. Kellogg, *J. Am. Chem. Soc.* **1985**, *107*, 3981, and references therein. For cyclic peptide analogues with potential biological activity, see: c) A. El-Hamid Attia, M. H. Abo-Ghalia, O. I. Abd El-Salam, *Collect. Czech. Chem. Commun.* **1994**, *59*, 1451; for amide catenanes, see: d) A. G. Johnston, D. A. Leigh, L. Nezhat, J. P. Smart, M. D. Deegan, *Angew. Chem.* **1995**, *107*, 1327; *Angew. Chem. Int. Ed. Engl.* **1995**, *34*, 1212; for metal ion-directed auto-assembly of cavitand architectures, see: e) L. Pirondini, D. Bonifazi, E. Menozzi, E, Wegelius, K. Rissanen, C. Massera, E. Dalcanale, *Eur. J. Org. Chem.* **2001**, 2311.

[22] a) T. Talik, Z. Talik, *Roczniki Chem.* **1962**, *36*, 539; b) T. Talik, *Roczniki Chem.* **1962**, *36*, 1049; c) T. Imahori, M. Uchiyama, T. Sakamoto, Y. Kondo, *Chem. Commun.* **2001**, 2450.

[23] A. Numata, Y. Kondo, T. Sakamoto, *Synthesis* **1999**, *2*, 306.

[24] K. Sonogashira, Y. Tohda, N. Hagihara, *Tetrahedron Lett.* **1975**, 4467.

[25] a) See reference [24]; b) A. Pelter, D. E. Jones, *J. Chem. Soc. Perkin Trans. 1* **2000**, 2289.

[26] The Eglinton/Galbraith ethyne coupling protocol has been widely employed for macrocyclisation reactions, see for example: L. Rossa, F. Vögtle, *Top. Curr. Chem.* **1983**, *113*, 72–75. Polypyridine ligands would be expected to exhibit a slightly lower propensity towards coordination polymer formation with $[Cu_2(OAc)_4]$ compared to CuCl, as the former copper salt has a lower number of available sites for additional ligand attachment.

[27] Interestingly, a red amorphous solid slowly precipitated from the reaction solution during the course of the $[Cu_2(OAc)_4]$ mediated

cyclisation of **12** in pyridine. It is possible that this solid was a network coordination polymer formed upon reaction between $[Cu_2(OAc)_4]$ and the **4** as it was generated.

[28] For an example of the use of semi-empirical AM1 calculations for successfully predicting the conformations of ethynyl macrocycles, see: a) M. Srinivasan, S. Sankararaman, H. Hopf, I. Dix, P. G. Jones, *J. Org. Chem*. **2001**, *66*, 4299. b) Retrieved from the CCSD.

[29] The metal salts and complexes used in the study were $CrCl_3 \cdot 6H_2O$, $FeCl_2$, $CoCl_2 \cdot 6H_2O$, $NiCl_2 \cdot 6H_2O$, $[PdCl_2(MeCN)_2]$, $[PtCl_2(MeCN)_2]$ and $[Cu(MeCN)_4]BF_4$. All remaining cations investigated were in the form of their anhydrous triflates. The chromium, iron, cobalt and nickel chlorides were each dissolved in a drop of distilled water prior to the preparation of the standard solutions in methanol to ensure complete solubility. For the same reason, the palladium and platinum complexes were initially dissolved in warm acetonitrile (1 mL) and in the former case diluted to the required volume with CH_2Cl_2. The $[Cu(MeCN)_4]BF_4$ solution was prepared in MeCN. The Cu^{II}, Ag^{I} and Tl^{I} triflates used were $\geq$ 99.9% purity.

[30] It may be noted that the UV/Vis spectra of the **4**/Ag^{I} solutions were very sensitive to the order of addition of the reactants and solvent. If the Ag^{I} and **4** were added first, then the solution immediately assumed a yellow colour with the concomitant development of a yellow precipitate. Upon subsequent dilution to the required volume with CH_2Cl_2 and MeOH, the precipitate and colouration persisted and produced irreproducible spectra. Reproducible results were obtained however, when the Ag^{I} solution was added first, followed by dilution to 3–4 mL with CH_2Cl_2 and MeOH, then addition of the ligand, and finally diluting to the required volume (5 mL) with CH_2Cl_2. Irreproducible UV/Vis spectra were also obtained with $Hg(CF_3SO_3)_2$ that had been prepared from the anion metathesis reaction between $HgCl_2$ and $AgCF_3SO_3$. The same problem was also encountered with commercial sources of $Hg(CF_3SO_3)_2$, which had probably been prepared by a similar route. Contaminating silver residues in the $Hg(CF_3SO_3)_2$ were presumably responsible for the latter observation. Reproducible results were finally obtained using $Hg(CF_3SO_3)_2$ that had been prepared from the reaction between HgO and $(CF_3SO_3)_2O$ in dry refluxing toluene, according to the procedure reported for the synthesis $Cu(CF_3SO_3)$; R. G. Salomon, J. K. Kochi, *J. Am. Chem. Soc.* **1973**, *95*, 3300.

[31] Proton-controllable fluorescence phenomena have been reported for linear, branched and cyclic conjugated organic scaffolds incorporating nitrogen-donor heterocycles, see: a) reference [16a]; b) R. E. Martin, J. A. Wytko, F. Diederich, C. Boudon, J.-P. Gisselbrecht, M. Gross, *Helv. Chim. Acta* **1999**, *82*, 1470; c) G. R. Pabst, O. C. Pfüller, J. Sauer, *Tetrahedron* **1999**, *55*, 5047; d) T. Yamamoto, K. Sugiyama, T. Kushida, T. Inoue, T. Kanbara, *J. Am. Chem. Soc.* **1996**, *118*, 3930. Macrocycle **4** and related structures are thus promising candidates for the construction of proton switches, transducers and conductors, as well as pH responsive NLO and electroluminescent materials.

[32] The reason why **11** shows slight but preferential binding to Al^{III}, Sc^{III} and In^{III} ions in dilute solution is currently unclear. It may however be related to the presence of the relatively electron-donating trimethylsilylethynyl groups in **11**, which would be expected to increase the basicity of the pyridine nitrogen lone pair electrons, thereby facilitating coordination to more highly charged metal ions.

[33] For a recent report of a ligand which signals the presence of Hg^{II} ions both by a colourimetric response and precipitation, see; O. Brümmer, J. J. La Clair, K. D. Janda, *Org. Lett*. **1999**, *1*, 415.

[34] Ligands **4** and **11** possess metal binding sites that are neither chelating or preorganised in any way. The fact that both ligands exhibit selective recognition of Hg^{II} and Pd^{II}, reflects the simple coordination environment, normally preferred by these two metals. This suggests that conjugated ligand structures based on **4** and **11** may serve as a new, lead class of sensory materials for metal ions with low coordination number preferences.

[35] Despite the fact that mercury is one of the most thoroughly studied heavy metal toxins, its influence as an environmental pollutant continues to be of deep concern. Within the global mercury cycle, the metal is ultimately biomethylated to the extremely toxic $MeHg^{+}$ ion, and concentrated inside living organisms. The enhanced toxicity of $MeHg^{+}$ stems from its lipophilic/hydrophilic character, which enables it to penetrate tightly constructed membrane partitions such as the blood-brain barrier. Mercury compounds impair the function of all proteins and enzymes whose activity relies upon metal coordinating, redox-active or conformation-determining cysteine groups. In the light of the aforementioned considerations, the discovery and development of new platforms for the detection and monitoring of Hg^{II} will continue to evoke considerable interest. For recent examples of fluorescence chemosensors for mercury, see: a) L. Prodi, C. Bargossi, M. Montalti, N. Zaccheroni, N. Su, J. S. Bradshaw, R. M. Izatt, P. B. Savage, *J. Am. Chem. Soc*. **2000**, *122*, 6769; b) Y.Shen, B. P. Sullivan, *J. Chem. Ed*. **1997**, *74*, 685; c) reference [18f].

[36] For the specific use of linear, ethynylpyridine-type ligands in the generation of coordination polymers, see: a) Md. B. Zaman, M. D. Smith, H.-Conrad zur Loye, *Chem. Commun*. **2001**, 2256; b) J. E. Fiscus, S. Shotwell, R. C. Layland, M. D. Smith, H.-Conrad zur Loye, U. H. F. Bunz, *Chem. Commun*. **2001**, 2674; c) A. Jouaiti, V. Jullien, M. Wais Hosseini, J.-M. Planeix, A. De Cian, *Chem. Commun*. **2001**, 1114; d) M. Maekawa, H. Konaka, Y. Suenaga, T. Kuroda-Sowa, M. Munakata, *J. Chem. Soc. Dalton Trans.* **2000**, 4160; e) A. J. Blake, N. R. Champness, A. Khlobystov, D. A. Lemenovskii, W.-S. Li, M. Schröder, *Chem. Commun*. **1997**, 2027.

[37] For a recent review on fluorescence molecular sensors for cation recognition, see: B. Valeur, I. Leray, *Coord. Chem. Revs.* **2000**, *205*, 3.

[38] For recent reviews on the metal ion directed approach to crystal engineering of coordination networks and hybrid frameworks, see: a) G. Férey, *Chem. Mater*. **2001**, *13*, 3084; b) M. Wais Hosseini, in *Crystal Engineering: From Molecules and Crystals to Materials*, (Eds.: D. Braga, F. Grepioni, G. A. Orpen), Kluwer, **1999**, pp.181–208. Macrocycle **4** and related structures may also potentially serve as tectons for the assembly of hydrogen-bonded polymers, zeolites and crystals. For the crystal engineering of 1D H-bonded polymers with ethynylpyridines, see: c) M. Ohkita, T. Suzuki, K. Nakatani, T. Tsuji, *Chem. Commun*. **2001**, 1454. For recent reviews on the design of organic solids through hydrogen-bond assembly, see: d) *Structure and Bonding* (Vol. Ed.: M. Fujita), **2000**, *96*, pp. 2–146; e) *Top. Curr. Chem*. **1998**, *198*, whole volume.

[39] For investigations into the potential use of multimetallic ethynylpyridyl scaffolds as molecular wires and multicentre magnetic materials, see: a) J. T. Lin, S.-S. Sun, J. J. Wu, L. Lee, K.-J. Lin, Y. F. Huang, *Inorg. Chem*. **1995**, *34*, 2323; b) A. J. Amoroso, A. M. W. Cargill Thompson, J. P. Maher, J. A. McCleverty, M. D. Ward, *Inorg. Chem*. **1995**, *34*, 4828. For the design of organic NLO materials with ethynylpyridines, see: c) reference [38c]. For a review on metal-coordinated conjugated pyridine ligands as NLO materials, see: d) H. Le Bozec, T. Renouard, *Eur. J. Inorg. Chem*. **2000**, 229. For the synthesis of linear ethynylpyridine-type metal complexes as potential NLO materials, see for example: e) J. T. Lin, M.-F. Yang, C. Tsai, Y. S. Wen, *J. Organomet. Chem*. **1998**, *564*, 257.

[40] For the use of ethynylpyridine-type ligands in the metal ion directed assembly of discrete supramolecular architectures, see: a) P. H. Dinolfo, J. T. Hupp, *Chem. Mater*. **2001**, *13*, 3113; b) C. J. Kuehl, S. D. Huang, P. J. Stang, *J. Am. Chem. Soc*. **2001**, *123*, 9634; c) K. R. Justin Thomas, J. T. Lin, Y.-Y. Lin, C. Tsai, S.-S. Sun, *Organometallics* **2001**, *20*, 2262.

[41] J. S. Brumbaugh, A. Sen, *J. Am. Chem. Soc*. **1988**, *110*, 803.

Received: November 7, 2002 [F4561]

